TECHNISCHE
UNIVERSITÄT
WIEN
Vienna University of Technology

UNIVERSITY OF
BELGRADE
Faculty of Mechanical
Engineering

XXIII INTERNATIONAL CONFERENCE ON "MATERIAL HANDLING, CONSTRUCTIONS AND LOGISTICS"

18th – 20th September, 2019

MHCL 2019

Edited by

Georg Kartnig, Nenad Zrnić and Srđan Bošnjak

VIENNA UNIVERSITY OF TECHNOLOGY (TU WIEN)
Institute for Engineering Design and Product Development

together with

UNIVERSITY OF BELGRADE
Faculty of Mechanical Engineering

VIENNA, AUSTRIA, 2019

INTERNATIONAL SCIENTIFIC COMMITTEE

Co-Chairmen:

Prof. Dr. Georg Kartnig, Vienna University of Technology, Austria
Prof. Dr. Nenad Zrnić, University of Belgrade, Serbia
Prof. Dr. Srđan Bošnjak, University of Belgrade, Serbia

Members of Scientific Committee:

Prof. Dr. Bogdevicius Marijonas, Vilnius Gediminas Technical University, Lithuania
Prof. Dr. Bojić Sanja, University of Novi Sad, Serbia
Prof. Dr. Bošnjak Srđan, University of Belgrade, Serbia
Prof. Dr. Ceccarelli Marco, University of Cassino, Italy
Prof. Dr. Chondros Thomas, University of Patras, Greece
Prof. Dr. Clausen Uwe, TU Dortmund, Fraunhofer Institute for Material Flow and Logistic, Germany
Prof. Dr. Ćuprić Nenad, University of Belgrade, Serbia
Prof. Dr. Czmochowski Jerzy, Wroclaw University of Science and Technology, Poland
Prof. Dr. Dentsoras Argiris, University of Patras, Greece
Prof. Dr. Dragović Branislav, University of Montenegro, Kotor, Montenegro
Prof. Dr. Dukić Goran, University of Zagreb, Zagreb, Croatia
Prof. Dr. Edl Milan, University of West Bohemia, Plzen, Czech Republic
Prof. Dr. Ekren Banu, Yaşar University, Turkey
Prof. Dr. Fottner Johannes, Technische Universität München, Germany
Prof. Dr. Furmans Kai, Karsruhe Institute of Technology, Germany
Prof. Dr. Gašić Milomir, University of Kragujevac, Kraljevo, Serbia
Prof. Dr. Gašić Vlada, University of Belgrade, Serbia
Prof. Dr. Georgiev Martin, Technical University Sofia, Bulgaria
Prof. Dr. Georgijević Milosav, University of Novi Sad, Serbia
Prof. Dr. Gerhard Detlef, Vienna University of Technology, Austria
Prof. Dr. Golder Markus, Technischen Universität Chemnitz, Germany
Prof. Dr. Guenthner Wilibald, TU Munich, Germany
Prof. Dr. Illes Bela, University of Miskolc, Hungary
Prof. Dr. Jančevski Janko, Ss. Cyril and Methodius University Skopje, Republic of Macedonia
Prof. Dr. Jerman Boris, University of Ljubljana, Slovenia
Prof. Dr. Jovanović Miomir, University of Niš, Serbia
Prof. Dr. Kartnig Georg, Vienna University of Technology, Austria
Prof. Dr. Katterfeld Andre, Otto-von-Guericke-Universitat Magdeburg, Germany
Prof. Dr. Kessler Franz, Montan University of Leoben, Austria
Prof. Dr. Kosanić Nenad, University of Belgrade, Serbia
Prof. Dr. Kreutzfeldt Jochen, Technische Universität Hamburg, Germany
Prof. Dr. Lerher Tone, University of Maribor, Slovenia
Prof. Dr. Markusik Sylwester, Silesian University of Technology, Gliwice, Poland
Prof. Dr. Mitrović Radivoje, University of Belgrade, Serbia
Prof. Dr. Ognjanović Milosav, University of Belgrade, Serbia
Prof. Dr. Oguamanam C.D. Donatus, Ryerson University Toronto, Ontario, Canada
Prof. Dr. Overmeyer Ludger, Leibniz University Hannover, Germany
Prof. Dr. Park Nam Kyu, Tongmyong Univ. of Information Technology, Busan, South Korea
Prof. Dr. Popović Vladimir, University of Belgrade, Serbia
Prof. Dr. Potrč Iztok, University of Maribor, Slovenia
Prof. Dr. Rakin Marko, University of Belgrade, Serbia
Prof. Dr. Rosi Bojan, University of Maribor, Slovenia
Prof. Dr. Rogić Miroslav, University of Banja Luka, Republic of Srpska, Bosnia and Herzegovina
Prof. Dr. Rusinski Eugeniusz, Wroclaw University of Science and Technology, Poland
Prof. Dr. Sari Zaki, University of Tlemcen, Algeria
Prof. Dr. Savković Mile, University of Kragujevac, Serbia
Prof. Dr. Sawodny Oliver, University of Stuttgart, Germany
Prof. Dr. Schmidt Thorsten, Dresden University of Technology, Germany
Prof. Dr. Schott Dingena, Delft University of Technology, The Netherlands
Prof. Dr. Sihn Wilfried, Vienna University of Technology, Fraunhofer Austria, Austria
Prof. Dr. Singhose William, Georgia Institute of Technology, Atlanta, USA
Prof. Dr. Solazzi Luigi, University of Brescia, Italy
Prof. Dr. ten Hompel Michael, TU Dortmund, Fraunhofer Institute for Material Flow and Logistic, Germany

Prof. Dr. Vidović Milorad, University of Belgrade, Serbia
Prof. Dr. Wehking Karl-Heinz, University of Stuttgart, Germany
Prof. Dr. Weigand Michael, Vienna University of Technology, Austria
Prof. Dr. Wimmer Wolfgang, Vienna University of Technology, Austria
Prof. Dr. Wypych Peter, University of Wollongong, Australia
Prof. Dr. Zrnić Nenad, University of Belgrade, Serbia

President of Honorary Scientific Committee and Conference Founder:

Prof. Dr. Đorđe Zrnić, University of Belgrade, Serbia

Members of Honorary Scientific Committee:

Prof. Dr. Babin Nikola, University of Novi Sad, Serbia
Prof. Dr. Hoffmann Klaus, Vienna University of Technology, Austria
Prof. Dr. Mijajlović Radić, University of Niš, Serbia
Prof. Dr. Oser Joerg, Graz University of Technology, Austria
Prof. Dr. Ostrić Davor, University of Belgrade, Serbia
Prof. Dr. Petković Zoran, University of Belgrade, Serbia
Prof. Dr. Severin Dietrich, Technical University of Berlin, Germany
Prof. Dr. Zrnić Đorđe, University of Belgrade, Serbia

ORGANIZING COMMITEE

Presidents of the Organizing Committee:

Prof. Dr. Georg Kartnig, Vienna University of Technology, Austria
Prof. Dr. Nenad Zrnić, University of Belgrade, Serbia

Vice President of the Organizing Committee:

Prof. Dr. Branislav Dragović, University of Montenegro, Montenegro

Members of Organizing Committee:

Prof. Dr. Gašić Vlada, University of Belgrade, Serbia
Assoc. Prof. Dr. Gnjatović Nebojša, University of Belgrade, Serbia
Alice Grano, Vienna University of Technology, Austria
Milojević Goran, University of Belgrade, Serbia
Đorđević Miloš, University of Belgrade, Serbia
Milenović Ivan, University of Belgrade, Serbia
Stefanović Aleksandar, University of Belgrade, Serbia
Urošević Marko, University of Belgrade, Serbia
Arsić Aleksandra, University of Belgrade, Serbia
Stanković Vlada, University of Belgrade, Serbia

Reviewers:

Prof. Dr. Bošnjak Srđan, Serbia
Prof. Dr. Dragović Branislav, Montenegro
Prof. Dr. Jerman Boris, Slovenia
Prof. Dr. Kartnig Georg, Austria
Prof. Dr. Lerher Tone, Slovenia
Prof. Dr. Zrnić Nenad, Serbia

Publisher:

University of Belgrade, Faculty of Mechanical Engineering

CIRCULATION: 100 copies

ISBN 978-86-6060-020-4

Alexander Haber
Research Assistant
Vienna University of Technology
Faculty of Mechanical and Industrial Engineering
Institute for Engineering Design and Product Development

Georg Kartnig
Professor
Vienna University of Technology
Faculty of Mechanical and Industrial Engineering
Institute for Engineering Design and Product Development

Development of a new DEM contact model for hygroscopic bulk solids

In this work, a contact model for the simulation of crystalline solid-bridges in discrete element method (DEM) programmes is presented and compared with previous so-called bond models. The aim of the contact model is a generally valid calibration covering all states of a hygroscopic bulk material in a silo. The developed simulation model is verified by qualitative sensitivity analysis. Furthermore, a procedure for easy calibration of the required model parameters is proposed.

Keywords: *DEM, caking, solid-bridge, bonds, hygroscopic bulk solid.*

1. INTRODUCTION

Even today, hygroscopic bulk solids such as fertiliser urea and other salts are mainly stored in storage sheds or domes, since their behaviour in silos remains challenging. Disadvantages often associated with dome-based storage include time-consuming dosing and mixing using the 'last-in-first-out' principle, sometimes carried out with wheel loaders. These issues lead to reduced product quality and significant economic losses every year. Computer-assisted analysis of bulk material behaviour by means of the discrete element method (DEM) could remedy this situation and provide the necessary data for designing process-safe silos. However, industry still lacks a suitable contact model for the simulation of hygroscopic bulk solids that can reproduce the unconfined yield strength achieved by solid-bridge formation under various operating conditions.

In [2] it is shown that a DEM contact model for hygroscopic bulk solids must reproduce the following properties in order to cover the entire parameter space of possible operating conditions for a given set of material parameters:

- strength as a function of moisture
- strength as a function of time
- strength as a function of pressure

The present article concretises and verifies the approach presented in [2]. Figure 9 illustrates this approach as a simulation scheme for the calculation of crystallisation-induced solid-bridges. In addition, we present a simple calibration procedure for determining the required model parameters.

2. EXISTING DEM COHESION MODELS FOR HYGROSCOPIC BULK SOLIDS

For the development of contact models for the DEM simulation, cohesive bulk solids can be divided into two groups based on the binding mechanism: reversible and irreversible consolidation.

Correspondence to: Dipl.-Ing. Alexander Haber
Faculty of Mechanical and Industrial Engineering,
Getreidemarkt 9, 1060 Vienna, Austria
E-mail: alexander.e307.haber@tuwien.ac.at

Reversible and an irreversible consolidation can be distinguished based on the time it takes for the formation of tensile forces acting between two neighbouring particles with respect to the duration of the simulation. In both groups, flow of the bulk solid can be caused only by exceeding the adhesion forces. If a bulk solid with reversible consolidation starts to flow, the formation of the corresponding adhesive forces takes place continuously during the simulation between neighbouring particles. This group includes cohesive powders with particles in the micro- to nanometer range, as well as moist bulk solids with particles up to the millimetre range. Corresponding to the large number of differerent binding mechanisms, a large number of contact models already exist for this group. These models are comparatively easy to implement, since in most cases the size of the adhesive forces is only a function of interparticle distance.

However, in the case of bulk solids with an irreversible binding mechanism, no adhesive force is formed between other particles when the adhesive forces are exceeded. The models developed for this purpose are so-called bond models and are used, for example, for chemical compound bulk solids with sinter bridges and hygroscopic bulk solids with crystalline solid-bridges, such as urea. The implementation in DEM programmes is a bit more complicated: In addition to the size of a possible adhesive force, the possible persistence of an upright connection between neighbouring particles must be determined. It should be noted that the term 'irreversible' applies only to typical simulation times of DEM simulations. Over typical real-world storage timescales, which go far beyond possible simulation timescales, consolidation can certainly occur via renewed formation of adhesive forces after previous breakage. A bond model implementation commonly used in DEM programmes is that for rocks after *Potyondy and Cundall* [6]. The input parameters required for this model are listed in Table 1.

Although bond models seem to be suitable for hygroscopic bulk solids in general, the implementation according to [6] is hardly applicable to industrial applications for designing a silo for urea, for example. In contrast to the model's workings in its original field of application, the dependence of solid-bridge strength on storage time and moisture content is strong for hygroscopic bulk solids. Therefore, the already complex

calibration of the models, in particular the bond radius, must be carried out each time under new operating conditions. Furthermore, the bond radius and thus the strength among all particles is assumed to be the same size, with local particle distances not considered.

Table 1. Input parameters for the classic bond model

		symbol	unit
particle parameters	particle diameter	d_P	m
	density	ρ	kg/m³
	elastic modulud	E	N/m²
	Poisson ratio	ν	-
interaction parameters without cohesion	coeff. of restitution	e	-
	sliding friction coeff.	μ	-
	rolling friction ceoff.	μ_r	-
bond parameters	bond radius	r_B	m
	bond range	a_{max}	m
	bond normal stiffness	k_N	N/m⁴
	bond shear stiffness	k_T	N/m⁴
	normal breaking stress	σ_{max}	N/m²
	shear breaking stress	τ_{max}	N/m²
	time of bond creation	t_{create}	s

In the following analysis, therefore, a bond model is presented that takes into account these dependencies of bulk solid pressure, moisture and storage time during the calibration process.

3. DEVELOPMENT OF A BOND MODEL FOR HYGROSCOPIC BULK SOLIDS

The principle of the new bond model has already been described in [2] (see Figure 9) and is based on the physical processes responsible for the formation of a crystalline solid-bridge. These processes occur in the following rough order:

1. Moisture exchange between the particles and the environment across particle surfaces
2. Capillary formation of liquid-bridges at contact points
3. Dissolution of the crystalline particulate solid
4. Formation of crystalline solid-bridges through complete evaporation or local supersaturation and crystal growth

The time scale for processes 3) and 4) is many times greater than that for processes 1) and 2). For detailed information, see [2] or [3].

The bond model takes effect only at a user-selected time t_{create}. At this time there is a random bed with various particle distances a. First, temporary liquid-bridge radii are calculated on the basis of the predetermined moisture content described by the liquid saturation S, from which bond radii are subsequently determined in accordance with the storage time $t_{storage}$. The required parameters are summarised in Table 2.

3.1 Calculation of the liquid-bridge radii

Depending on the amount of liquid contained in a bulk material, different saturation regimes and different types of liquid-bridges between the particles can be distinguished. The amount of liquid is expressed in terms of the pore volume occupied by the liquid saturation S.

$$S = \frac{V_{Flüssig}}{V_{Poren}} = \frac{V_{Flüssig}}{\varepsilon \cdot V_{Gesamt}} \quad (1)$$

Table 2. Input parameters for the hygroscopic bond model

		symbol	unit
moisture parameters	bulk saturation	S	-
	bulk porosity	ε	-
	contact angle	δ	rad
	bond range	a_{max}	m
time parameters	time of bond creation	t_{create}	s
	crystallisation parameter	t_{63}	h
	Storage time	$t_{storage}$	h
material parameters	bond normal stiffness	k_N	N/m³
	bond shear stiffness	k_T	N/m³
	normal breaking stress	σ_{max}	N/m²
	shear breaking stress	τ_{max}	N/m²

In (1), ε describes the porosity of the bulk solid. In the so-called pendular-state, i.e., the range of $S_{min} < S < 0.08$, liquid-bridges occur exclusively in the form of individual annular bridges (see Figure 1). The minimum moisture at which the bulk solid loses its cohesive properties is stated in [4] as $S_{min} = 0.002$. In the funicular-state $0.08 < S < 0.24$, the bulk solid gradually achieves union of individual bridges into more complex structures. Although the global connection of liquid-bridges in both cases is interrupted by pores, liquid can be exchanged along the particle surfaces via channels in the size range of the roughness itself [4].

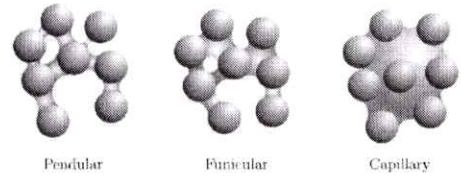

Figure 1. Liquid-bridges at different saturation regimes [11]

In the equilibrium state, therefore, capillary pressures are similar to one another across all liquid-bridges due to liquid exchange [8], if the influences of surface tension and gravitational acceleration are neglected. According to *Pietsch and Rumpf* [7], the radii, the volumes and the capillary pressures of the liquid-bridges can be calculated given known particle diameter d_P, particle distance a, filling angle β and contact angle δ (see Figure 2).

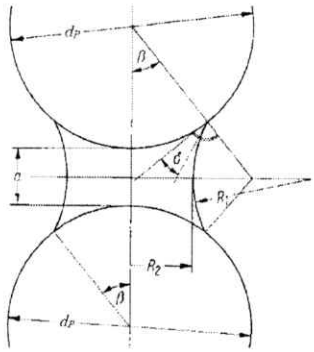

Figure 2. Liquid-bridge model [7]

With complete wetting, the contact angle δ is 0°, so the liquid-bridges connect tangentially to the particles.

In order to determine the equilibrium local liquid-bridge radii, a target value for the capillary pressure as a function of liquid saturation must be obtained. To this end, a mean filling angle $\bar{\beta}$ is first calculated on the basis of the empirical equation presented in [12]:

$$\bar{\beta} = \arcsin\left[\left(\frac{S}{0{,}36}\frac{\varepsilon^2}{1-\varepsilon}\frac{1}{C_a}\frac{1}{C_\delta}\right)^{1/4}\right] \tag{2}$$

This equation provides an explicit relationship for $\bar{\beta} = \mathrm{f}(S, \varepsilon, a, d_P, \delta)$ with the correction functions C_a and C_δ, which can be omitted for $a = 0$ and $\delta = 0$

$$C_a = 1 + 6\frac{a}{d_P} \tag{3}$$

$$C_\delta = 1 + 1{,}1\sin\delta \tag{4}$$

Eq. (2) is in good agreement with *Pietsch and Rumpf*'s [7] general model, in which β cannot be represented in explicit form for a monodisperse bulk solid in the range $0.05 \le S \le 0.3$. Although nonpenetration of neighbouring particles ($a > 0$) is considered, several DEM simulations have shown that the average particle distance $\bar{a}$ remains less than zero. Therefore the correction factor C_a need not be taken into account for the calculation of $\bar{\beta}$.

According to the Young-Laplace equation

$$p_K = \gamma_l\left(\frac{1}{R_1} + \frac{1}{R_2}\right) \tag{5}$$

with liquid surface tension γ_l and the required radii according to [7]

$$R_1 = \frac{d_P(1-\cos\beta) + a}{2\cos(\beta+\delta)} \tag{6}$$

$$R_2 = \frac{d_P}{2}\sin\beta + R_1[\sin(\beta+\delta) - 1], \tag{7}$$

the dimensionless positive capillary pressure F_{pK} can be calculated if R_2 takes a negative sign in (5):

$$F_{pK} = p_K\frac{d_P}{\gamma_l} \tag{8}$$

The liquid surface tension γ_l therefore does not need to be determined.

The local filling angles β and liquid-bridge radii R_2 are calculated as a function of the particle distance a for a given dimensionless capillary pressure F_{pK}.

Since an explicit equation for β according to *Pietsch and Rumpf* [7] is not possible, (2) would seem to be an obvious source for the calculation of the local filling angles. However, Figure 3 shows that there is not sufficient agreement between the analytic equation and the empirical equation using the correction factor C_a (3).

As can be seen in Figure 4, on the other hand, the analytic function can be very well approximated by the following cubic function:

$$\frac{a}{d_P} = A\bar{\beta}^3 + B\bar{\beta}^2 + C\bar{\beta} \tag{9}$$

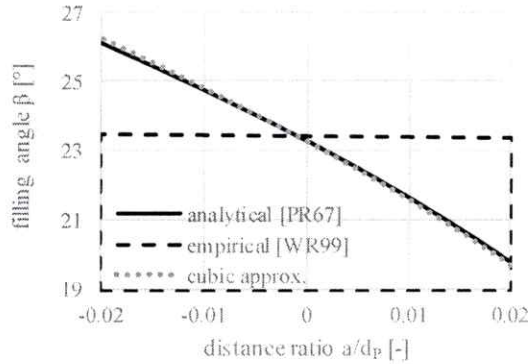

Figure 3. Dependence of the filling angle on the distance ratio for various approaches (S=0.05, ε=0.34, δ=0 → F_{pK}=16.745)

Therein, the coefficients are determined by empirical equations as functions of F_{pK}:

$$A = 2{,}1\cdot10^{-9}{F_{pK}}^2 + 4\cdot10^{-7}F_{pK} - 2{,}2\cdot10^{-6} \tag{10}$$

$$B = -1\cdot10^{-7}{F_{pK}}^3 + 3{,}6\cdot \cdot 10^{-6}{F_{pK}}^2 - 6\cdot10^{-5}F_{pK} - 4\cdot10^{-5} \tag{11}$$

$$C = \left[3{,}5\cdot10^{-5}{F_{pK}}^2 - 0{,}0097\right]e^{\left(-\frac{a}{6d_P}+1\right)} - \left[2{,}1\cdot10^{-9}{F_{pK}}^2 - 2{,}1\cdot \cdot 10^{-9}{F_{pK}}^2 - 0{,}0084\right]e^{\left(-\frac{a}{6d_P}\right)} \tag{12}$$

Eq. (9) is written by transformation as a reduced cubic equation without a quadratic term and then solved for β [°] by applying Cardano's method.

According to Figure 4, equations (9) - (12) provide a very good approximation for (5) or rather (8) in a range of $0.1 \le F_{pK} \le 18$. The range specified for the dimensionless capillary pressure F_{pK} covers the entire range of validity of the liquid saturation of $0.05 \le S \le 0.3$ for a realistic bulk solid porosity of $\varepsilon \approx 0.3 - 0.5$. The liquid saturation range is limited by the underlying model of individual annular bridge occurrences. Since the approximation currently contains no dependence on the contact angle δ, this work applies exclusively to $\delta = 0$.

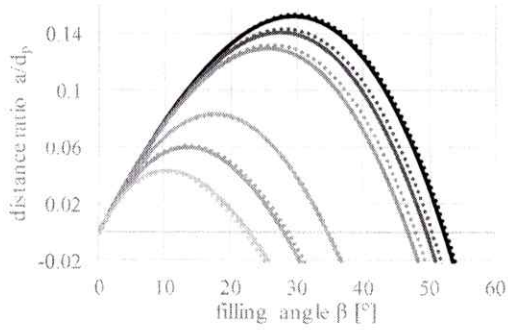

Figure 4. Curve family f(F_{pK}, β, a/d_P). Comparison between [7] and by the cubic function (9) in the validity range of the developed contact model

With the local filling angles determined, the liquid-bridge radii R_2 are calculated according to (7).

3.2 Calculation of bond radii

On the basis of the determined liquid-bridge radii and the storage time to be investigated, the bond radii R_B can be calculated using the time parameter t_{63} according to *Tomas* [9]:

$$R_B = R_2 \cdot \left[1 - e^{\left(-\frac{t_{storage}}{t_{63}}\right)}\right] \tag{13}$$

According to (13), crystallisation growth is determined by an inverse exponential function. Therein t_{63} describes the time at which the crystallisation progress reaches 63%. For very long storage timescales, the bond radius corresponds to the liquid-bridge radius. Depending on the solubility L of the particulate solid in the liquid, a more or less porous bond cross-section is formed during crystallisation. This circumstance is taken into account by the calibration of the breaking stress in accordance with Chapter 4. Since the solubility L can be strongly temperature-dependent (see Table 3), a direct consideration of this parameter in (13) is possible:

$$R_B = L \cdot R_2 \cdot \left[1 - e^{\left(-\frac{t_{storage}}{t_{63}}\right)}\right] \tag{14}$$

When using (14) instead of (13), the calibrated breaking stress takes on a different value, and temperature dependence is taken into account by the actual solubility.

Table 3. Solubility of urea in water as a function of temperature [5]

	temperature [°C]					
	0	20	40	60	80	100
L [g/g]	0.65	1.07	1.65	2.53	4.05	7.40

4. CALIBRATION OF MODEL PARAMETERS

To carry out a DEM simulation with the presented contact model, the parameters listed in Table 2 must be set. As with the parameters in Table 1, the liquid saturation S and the storage time $t_{storage}$ must now be specified instead of directly defining the unknown bond radius.

The liquid saturation of the bulk solid can be determined by means of so-called sorption isotherms from the relative humidity RH and the ambient temperature T_U. Table 4 shows some values of the sorption isotherm of urea at 25 °C.

Table 4. Sorption isotherm values for urea at 25 °C [1]

	relative humidity RH [%]					
	12	33	53	76	92	97
X [%]	0.09	0.11	0.11	0.67	49.37	58.50

Therein, X is mass-based material moisture, mostly used for sorption isotherms

$$X = \frac{m_{liquid}}{m_{particle,dry}}\ , \tag{15}$$

which can be easily converted into the liquid saturation S required as input parameter:

$$S = X \cdot \frac{1-\varepsilon}{\varepsilon} \cdot \frac{\rho_{particle}}{\rho_{liquid}} \tag{16}$$

The typical progression of sorption isotherms according to Table 4 shows at first a very small amount of adsorbed liquid and a strong increase in moisture from a critical relative humidity CRH.

The bulk porosity ε can be obtained in many cases from the results of a first simulation without bonds. However, if the particle size selected in the simulation does not correspond to the actual grain size, this is not possible and the parameter ε must then be calibrated. This case will not be discussed here. However, a possible procedure for its calibration could be a final comparison of the calculated liquid-bridge volume with the adjusted liquid saturation according to (1).

The physical value of the contact angle δ must be determined in accordance with the wettability of the bulk solid with the surrounding liquid. Therefore, a calibration is not required.

For the bond range a_{max}, a relatively large value can be selected. Since no unphysical results are allowed while determining the correct solution of the cubic equation, no liquid-bridge will be created unless the capillary pressure at that distance reaches the desired target value, even if the value for a_{max} is large. In this sense, a_{max} only defines the range of possible contact partners. For many cases, a_{max} can be chosen in a range of $0.02 \leq a_{max}/d_P \leq 0.05$.

The time for the creation of the bonds t_{create} is chosen by the user on the basis of the simulation process so that the particle bed has already come to rest and the kinetic energy is close to zero.

Since crystalline solid-bridges consist of the same material as the particles themselves, the same stiffness settings can be used for the bond stiffnesses k_N and k_T as for the cohesionless particle contact model. If the elastic modulus is used to quantify particle stiffness, it can be converted into the required stiffness per unit area [N/m³] as follows:

$$k = \frac{E}{L_0} \tag{17}$$

with

$$L_0 \approx d_P \quad \text{for} \quad k_N \quad \text{and} \tag{18}$$

$$L_0 \approx 2R_B \quad \text{for} \quad k_T \tag{19}$$

Finally, the breaking stresses σ_{max} and τ_{max} and the crystallisation parameter t_{63} remain from Table 2 for the calibration. Since studies on single grains (e.g., [10] and [3]) are generally very complex, the uniaxial compression test is used here and it must be carried out twice. For this purpose, the sample material is prepared identically in both cases with respect to liquid saturation and temperature. Subsequently, the samples are precompressed by pressure from above and stored in a climate chamber under defined conditions. In the last step, the walls of the mostly cylindrical sample geometry are removed, and the sample is crushed by loading from above. Based on the maximum applied force and the cross-section of the sample, the compressive strength σ_c is determined.

The first sample is stored as long as the crystallisation process is complete, at which point no further increase in compressive strength is to be expected with further storage (Figure 5). The stress value σ_1 determined at t_1 serves to calibrate the maximum breaking stresses σ_{max} and τ_{max}.

The heretofore unknown parameter t_{63} required for the calibration simulations must be determined first. This is done using the second sample shown in Figure 5, which is stored for only a few hours. The exact storage time t_2 depends on the bulk solid and the added liquid. The goal is the determination of a representative point σ_2 on the solidification curve for the determination of t_{63} with:

$$t_{63} = -\frac{t_2}{\ln\left(1 - \frac{\sigma_2}{\sigma_1}\right)} \tag{20}$$

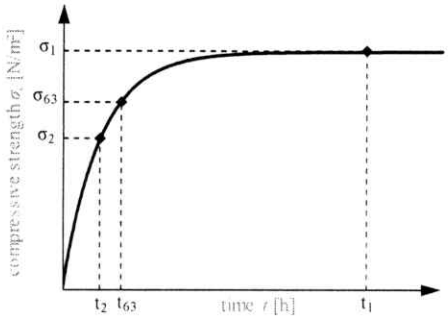

Figure 5. Consolidation curve for calibration of the bond model by means of a uniaxial compression test

5. VERIFICATION AND VALIDATION

To verify the developed contact model, we simulate a uniaxial pressure test, and we then qualitatively assess the compressive strengths achieved at different precompactions, liquid saturations and storage times. For this purpose, particles with a uniform diameter of 6 mm are filled into a virtual sample cylinder. The cylinder has a diameter of 61 mm and a height of 85 mm. Figures 6, 7 and 8 show the results of these simulations.

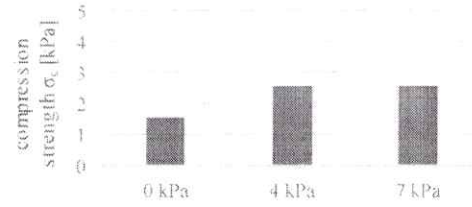

Figure 6. Compressive strength as a function of compression pressure at $t_{storage} = t_{63}$ and $S = 0.3$.

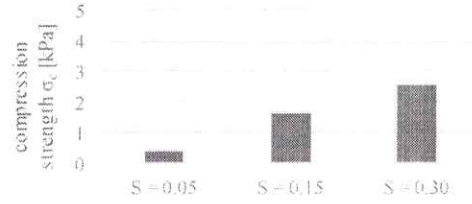

Figure 7. Compressive strength as a function of liquid saturation at 4 kPa and $t_{storage} = t_{63}$.

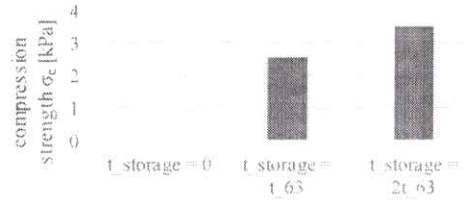

Figure 8. Compressive strength as a function of storage time at 4 kPa and $S = 0.3$.

According to Figure 6, a dependence on compression pressure is evident only at very low pressures. This restriction corresponds to the range over which particles rearrange from a loose bed to a dense packing. Further reduction of interparticle distance is relatively minor in comparison. Under typical silo pressures, this dependence is observed to be rather low, coinciding with the observations of *Wahl et al.* [10].

The trend in compressive strength as a function of liquid saturation and storage time (Figures 7 and 8) is in line with expectations. A detailed validation by comparative measurements is still pending.

6. CONCLUSION

A DEM contact model for hygroscopic bulk solids was developed. An essential feature is its dependence on storage time and moisture. With a one-time calibration, a parameter set valid for all operating conditions can be found. With the help of the presented calibration method, all required parameters can be determined with a simple test bench and little effort. Verification of the model was based on various parameter variations, yielding promising behaviour.

In the next step, the model for various hygroscopic bulk solids, such as urea, sugar, etc., is calibrated. Subsequently, the simulation results are compared with comprehensive measurement series.

Future steps also include an extension of the model with regard to the following possibilities:

- Consideration of a possible particle size distribution
- Detection of contact angles $\delta \neq 0°$
- Impact of local humidity and temperature differences

REFERENCES

[1] Bröckel, U., Kirsch, R., Wahl, M. and Feise, H. J.: Formation and strength of solid bridges in bulk solids, Particulate Science and Technology, Vol. 26, No. 1, pp. 23-32, 2007.

[2] Haber, A. and Kartnig, G.: Ansätze zur Berücksichtigung der zeit- und ortsabhängigen Eigenschaften von Festkörperbrücken in DEM-Simulationen, Logistics Journal: Proceedings, 2018.

[3] Kirsch, R., Williams, R., Bröckel, U., Hammond, R. and Jia, X.: Direct Observation of the Dynamics of Bridge Formation between Urea Prills, Industrial & Engineering Chemistry Research, Vol. 50, No. 20, pp. 11728–11733, 2011.

[4] Lukyanov, A.V., Sushchikh, M.M., Baines, M.J. and Theofanous, T.G.: Superfast nonlinear diffusion: Capillary transport in particulate porous media, Physical review letters, Vol. 109, No. 21, pp. 214501, 2012.

[5] Meessen, J. H.: Urea, Ullmann's Encyclopedia of Industrial Chemistry, pp. 657-695, 2012.

[6] Potyondy, D.O. and Cundall, P.A.: A bonded-particle model for rock, International journal of rock mechanics and mining sciences, Vol. 41, No. 8, pp. 1329-1364, 2004.

[7] Pietsch, W. and Rumpf, H.: Haftkraft, Kapillardruck, Flüssigkeitsvolumen und Grenzwinkel einer Flüssigkeitsbrücke zwischen zwei Kugeln, Chemie Ingenieur Technik, Vol. 39, No. 15, pp. 885-893, 1967.

[8] Schaber, M: *Flüssigkeitsumverteilung in feuchten Granulaten, Dissertation, Universität des Saarlandes*, Fakultät für Naturwissenschaften und Technik, Saarbrücken, 2015.

[9] Tomas, J.: Zur Verfestigung von Schüttgütern – Mikroprozesse und Kinetikmodelle, Chemie Ingenieur Technik, Vol. 69, No. 4, pp. 455-467, 1997.

[10] Wahl, M., Kirsch, R., Bröckel, U., Trapp, S. and Bottlinger, M.: Caking of Urea Prills, Chemical Engineering & Technology, Vol. 129, No. 6, pp. 674–678, 2006.

[11] Washino, K., Chan, E. L., Midou, H., Tsuji, T. and Tanaka, T.: Tangential viscous force models for pendular liquid bridge of Newtonian fluid between moving particles, Chemical Engineering Science, Vol. 174, pp. 365-373, 2017.

[12] Weigert, T. and Ripperger, S.: Calculation of the liquid bridge volume and bulk saturation from the half-filling angle, Particle & Particle Systems Characterization, Vol. 16, No. 5, pp. 238-242, 1999.

NOMENCLATURE

a	[m]	particle distance
d_P	[m]	particle diameter
F_{pK}	[-]	dimensionless capillary pressure
k_N	[N/m³]	bond normal stiffness
k_T	[N/m³]	bond shear stiffness
L	[g/g]	solubility
p_K	[Pa]	capillary pressure
R_2	[m]	liquid-bridge radius
R_B	[m]	bond radius
S	[-]	liquid saturation
t_{63}	[h]	crystallisation parameter
$t_{storage}$	[h]	storage time
X	[g/g]	mass-based material moisture

Greek symbols

β	[rad]	filling angle
$\bar{\beta}$	[rad]	mean filling angle
δ	[rad]	contact angle
ε	[-]	bulk porosity
σ_c	[N/m²]	compression strength
σ_{max}	[N/m²]	normal breaking stress
τ_{max}	[N/m²]	shear breaking stress

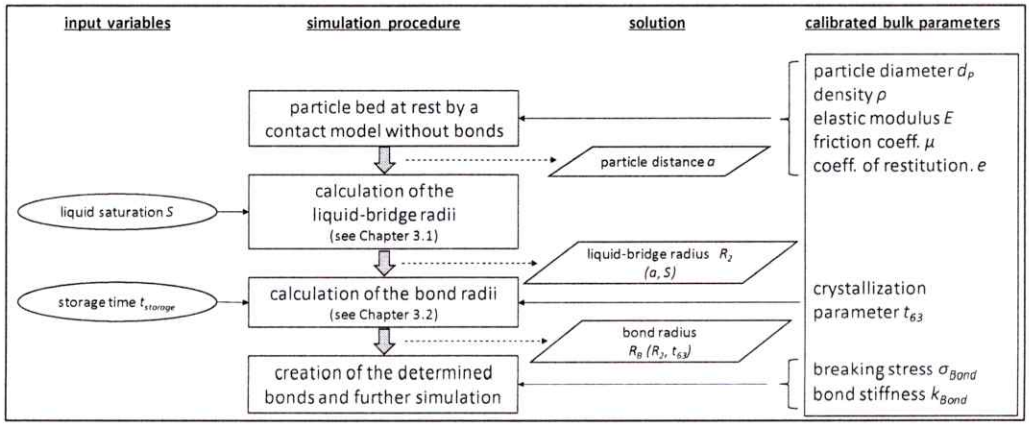

Figure 9. Simulation procedure for consideration of pressure- and time-dependent solid-state bridges [2]